Energies **2015**, *8*, 4237-4252; doi:10.3390/en8054237

OPEN ACCESS

energies

ISSN 1996-1073

www.mdpi.com/journal/energies

Article

Enhanced Hydrogen Generation Properties of MgH_2-Based Hydrides by Breaking the Magnesium Hydroxide Passivation Layer

Liuzhang Ouyang [1,2], Miaolian Ma [1], Minghong Huang [1], Ruoming Duan [1], Hui Wang [1,2], Lixian Sun [3] and Min Zhu [1,2,*]

[1] School of Materials Science and Engineering and Key Laboratory of Advanced Energy Storage Materials of Guangdong Province, South China University of Technology, Guangzhou 510641, China; E-Mails: meouyang@scut.edu.cn (L.O.); miaolianma@163.com (M.M.); h.minghong@mail.scut.edu.cn (M.H.); meduanrm@gmail.con (R.D.); mehwang@scut.edu.cn (H.W.)

[2] China-Australia Joint Laboratory for Energy & Environmental Materials, South China University of Technology, Guangzhou 510641, China

[3] Guangxi Collaborative Innovation Center of Structure and Property for New Energy and Materials, Guilin 541004, China; E-Mail: lxsun@dicp.ac.cn

* Author to whom correspondence should be addressed; E-Mail: memzhu@scut.edu.cn; Tel.: +86-20-8711-3924; Fax: +86-20-8711-2762.

Academic Editor: Craig M. Jensen

Received: 28 February 2015 / Accepted: 4 May 2015 / Published: 11 May 2015

Abstract: Due to its relatively low cost, high hydrogen yield, and environmentally friendly hydrolysis byproducts, magnesium hydride (MgH_2) appears to be an attractive candidate for hydrogen generation. However, the hydrolysis reaction of MgH_2 is rapidly inhibited by the formation of a magnesium hydroxide passivation layer. To improve the hydrolysis properties of MgH_2-based hydrides we investigated three different approaches: ball milling, synthesis of MgH_2-based composites, and tuning of the solution composition. We demonstrate that the formation of a composite system, such as the MgH_2/LaH_3 composite, through ball milling and *in situ* synthesis, can improve the hydrolysis properties of MgH_2 in pure water. Furthermore, the addition of Ni to the MgH_2/LaH_3 composite resulted in the synthesis of LaH_3/MgH_2/Ni composites. The LaH_3/MgH_2/Ni composites exhibited a higher hydrolysis rate—120 mL/(g·min) of H_2 in the first 5 min—than the MgH_2/LaH_3 composite—95 mL/(g·min)—without the formation of the magnesium hydroxide passivation layer. Moreover, the yield rate was controlled by manipulation of the particle size via ball milling.

The hydrolysis of MgH_2 was also improved by optimizing the solution. The MgH_2 produced 1711.2 mL/g of H_2 in 10 min at 298 K in the 27.1% ammonium chloride solution, and the hydrolytic conversion rate reached the value of 99.5%.

Keywords: MgH_2-based hydride; hydrolysis; hydrogen generation; composites

1. Introduction

The global energy crisis and our current ecological problems have stimulated the development of new clean energies [1–4]. Hydrogen has a high energy density of 142 MJ/kg, three times higher than that of petroleum, with 47 MJ/kg [5,6]. Upon combustion, the byproduct is water, which can subsequently be used to regenerate hydrogen [7–10]. Therefore, hydrogen is regarded as a potential candidate for clean and sustainable fuel to replace fossil fuels [11–13]. Currently, hydrogen is primarily produced through the processing of fossil fuels, biomass and water. The main methods include fossil fuel reforming [14], biological hydrogen production [15], generating hydrogen from water decomposition [16] and hydrogen production by metal or hydride hydrolysis [17]. Fuel processing of methane is the most common hydrogen production method in commercial use today [18,19]. Biohydrogen technologies include direct biophotolysis [20–22], indirect biophotolysis [23], photo-fermentation [24,25], and dark-fermentation [26–28]. Electrolysis technology is an effective method for transforming electrical energy into chemical energy and can be traced back to 1890 [29–31]. Photocatalytic decomposition of water was first used by Fujishima and Honda [32] and the catalytic efficiency reached 93% under the UV irradiation [33,34].

In recent years, more and more attention has been paid to hydrogen generation by hydrolysis of metals or metal hydrides for their high theoretical hydrogen yield. The main hydrogen generation metals include Al and Mg alloys, due to their light weight, abundance, and low cost and the byproduct being benign. The self-corrosion of hydrogen evolution reactions of aluminum has led to many studies focusing on hydrogen generation with aluminum and its alloys. However, aluminum has a strong affinity for oxygen, in the form of a dense oxide layer formed on the surface of aluminum and its alloys, making the corrosion potential shift nearly 1 V in the positive direction, thereby interrupting the corrosion reaction of aluminum [35]. This becomes the major challenge to realizing continuous hydrogen generation through aluminum corrosion. How to remove or prevent the formation of a dense aluminum oxide layer is the key issue in the hydrogen generation process by hydrolysis of aluminum alloys. Many methods have been reported to improve the hydrolysis properties of aluminum as, for example, changing the reaction solution (alkali solution, $NaAlO_2$ solution, Na_2SnO_3 solution, *etc.*) [36–38] and improving the reaction activity of aluminum alloys by ball milling and/or some special metal doping [39–41]. However, the corrosion of equipment in alkali or salt solution and the risk of corrosion of materials restrict its commercial utilization. Additional research is still needed to further improve the hydrogen generation performance with Al alloys. The hydrolysis reaction of Mg is rapidly interrupted because of the formation of a passive magnesium hydroxide layer.

Compared with pure metals or alloys, the metal hydrides can generate double the amount of hydrogen by hydrolysis, and the generated high purity hydrogen can be passed directly into the cells as fuel [42].

In addition, the fuel cell-generated water could be recycled and used for hydrolysis, thus achieving reduced weight of the system. Due to the hydrogen generation by hydrolysis having the excellent properties of widely raw material sources, high hydrogen generation yield, high hydrogen purity, and environmental friendliness, a large amount of metal hydrides have been studied as the mobile hydrogen source of fuel cell, such as LiH [43], CaH_2 [44], MgH_2 [45–48], $NaBH_4$ [49–51], $LiBH_4$ [52,53], $LiAlH_4$ [42,52]. Among them, LiH, CaH_2, and $LiAlH_4$ can react with water violently, so the uncontrollable reaction leads to poor practicability. Among these methods, production of hydrogen using $NaBH_4$ is safety and controllability, but the regeneration of $NaBH_4$ needs a great deal of energy leading to a higher cost. On the other hand, the efficiency and service life of the catalyst and the price of the whole system restrict the promotion and application of $NaBH_4$ hydrogen production technology. Therefore, looking for a cheap and practical technology to generate hydrogen always is a fervent focus of research all over the world. Comparing the hydrolysis of MgH_2 with that of $NaBH_4$, it is not necessary for a highly basic solution to stabilize the $NaBH_4$, whereas MgH_2 can generate hydrogen in the absence of a catalyst at room temperature. Furthermore, as the existence of $Mg(OH)_2$, the hydrolysis product could be easily recycled. In comparison to ammonia borane (AB), there is no requirement for a catalyst to improve the hydrolysis rate, only an adjustment to the particle size or solution, which influence hydrolysis rate and hydrogen yield.

MgH_2-based materials have higher theoretical hydrogen content (15.2%) and Mg element is abundant in the earth's crust (2.4%). They are low cost, have a high hydrogen yield, and are gentle on the environment, making them a potential candidate for high-quality hydrogen generation material. The progress of reaction can be concluding as in Equation (1):

$$MgH_2 + 2H_2O = Mg(OH)_2 + 2H_2\ \Delta H^{\theta}(298K) = -134.325\ KJ/mol \cdot H_2 \quad (1)$$

The hydrolysis production of MgH_2-based hydride ($Mg(OH)_2$) is harmless to the environment and easily reused and recycled [54]. Fortunately, the hydrolysis reaction of MgH_2 occurred immediately when it had contact with water at room temperature. However, the hydrolysis reaction of MgH_2 is rapidly interrupted because of the formation of a passive magnesium hydroxide layer, which prevents the diffusion of the water to the particle inside, so that the hydrolysis reaction after the early high-speed reaction stage is quickly stagnated.

In order to improve the hydrolysis efficiency and the reaction rate, the main methods such as ball milling, alloying, changing hydrolysis solution composition, catalyst introduction, *etc*. were adopted. Research has shown that although adding acid to form Mg^{2+} ion is an effective method, it may pollute the environment, introduce an additional hazard to the equipment, and lower overall safety [55,56]. The addition of CaH_2 appears to be very promising, but this reagent is too reactive and needs an extended milling time of 10 h that is not propitious for industrial production in terms of feasibility and safety [57]. In addition, hydrolyses of high-energy ball-milled MgH_2 composites in aqueous NaCl solution [58–60], aqueous KCl solution [61], or in different alcoholic solutions [62] have been used to produce hydrogen, but the state-of-the-art hydrolysis performance is still far from commercial utilization. Even when Ni was added to MgH_2 in KCl solution, the hydrolysis reaction did not show any significant reactivity improvement [61]. Recently, ultrasonication has been shown to enhance hydrogen generation during the hydrolysis process of magnesium hydride, but it has the disadvantages of requiring extra ultrasonic equipment and the associated extra energy consumption [63]. Therefore, the key issue relating to MgH_2

hydrolysis remains the circumvention of the barrier of oxide/hydroxide layer formation during the hydrolysis process so as to realize complete hydrolysis [47,64]. In this paper, we review our recent research results about hydrolysis of MgH_2-based hydrides and confirm the effect of the ball-milling and catalyst-introducing methods to break the magnesium hydroxide passivation layer to enhance the hydrolysis rate and hydrogen generation yield. The hydrolysis rate and yield in the pure water of *in situ* synthetic MgH_2-based composites could be further adjusted by controlling the particle size via ball milling. The ammonium chloride solution can destroy the $Mg(OH)_2$ passivation layer and accelerate the hydrolysis process of MgH_2, which can produce 1711.2 mL/g hydrogen in 10 min at 298 K with a hydrolytic conversion rate of 99.5% in the 27.1% ammonium chloride solution. Moreover, the optimization of the $MgCl_2$ aqueous solution was also investigated. It not only eliminates the introduction of impure gas and byproduct, but also simplifies the regeneration process. Such a result opens a promising route for improving hydrolysis properties for commercial hydrogen production.

2. Experimental

2.1. Sample Preparation

The reagent of MgH_2 was purchased from Sigma-Aldrich Inc. The rare earth ingot was broken into small particles and filtered through a 400-mesh sieve, then hydrogenated at 573 K for 4 h with the hydrogen pressure of 4 MPa by using an AMC gas reaction controller (Advance Materials Corporation, Pittsburgh, PA, USA) to prepare REH_3 hydride. The MgH_2 was ball milled under hydrogen atmosphere for 3 h using QM-3SP4 planetary ball mill (Nanjing NanDa Instrument Plant, Nanjing, China) with a ball-to-powder mass ratio of 20:1 at rotational speed of 500 rpm. The MgH_2/REH_3 composite was obtained by ball milling LaH_3 and MgH_2 with different atomic ratios of 3:1, 5:1, 8.5:1 under hydrogen atmosphere for 4 h. The ball milling was performed on a QM-3SP4 planetary ball mill rotating at 500 rpm with the ball-to-powder mass ratio of 20:1. To prevent samples and raw materials from oxidation and/or hydroxide formation, all samples were stored and handled in an Ar filled glove box. The solution of $MgCl_2$ and NH_4Cl was prepared to be used as hydrolysis solution: 2.38 g $MgCl_2$ was dissolved into 500 mL deionized water to form a solution of 0.5 mol/L $MgCl_2$. 4.7 g, 9.3 g, 18.6 g and 37.2 g NH_4Cl were dissolved into 100 mL of deionized water to form solutions with the mass ratio of 4.5%, 8.5%, 15.7%, and 27.1%, respectively.

2.2. Hydrolysis Experiment

The hydrolysis reactions of the MgH_2 or MgH_2/LaH_3 composite were carried out in a 250 mL Pyrex glass reactor with three openings, one for water addition, one for hydrogen exhausting and one for inserting the thermometer. All the experiments were carried out at room temperature (298 K), without external heating. Figure 1 shows the schematic hydrolysis reaction equipment which was used to quantify the hydrogen production rate and yield. Samples of 0.1–0.2 g were added into the Pyrex glass, before 20 mL water or $MgCl_2$ solution were added to react with the alloys. Hydrogen production reaction started when the alloys contacted with pure water or solution. The generated hydrogen was exhausted through a Tygon tube, then passed through a Monteggia washing bottle filled with water at room temperature in order to condense the water vapor, and collected hydrogen by extracting water in a beaker

which was put on an electronic scales to recorded the weight changes over time, in order to measure the quantity of hydrogen. The hydrogen generation rate and yield can be calculated from the reaction time and hydrogen volume, which was measured and analyzed by the computer. Each experiment test was repeated at least two times in order to confirm its reproducibility.

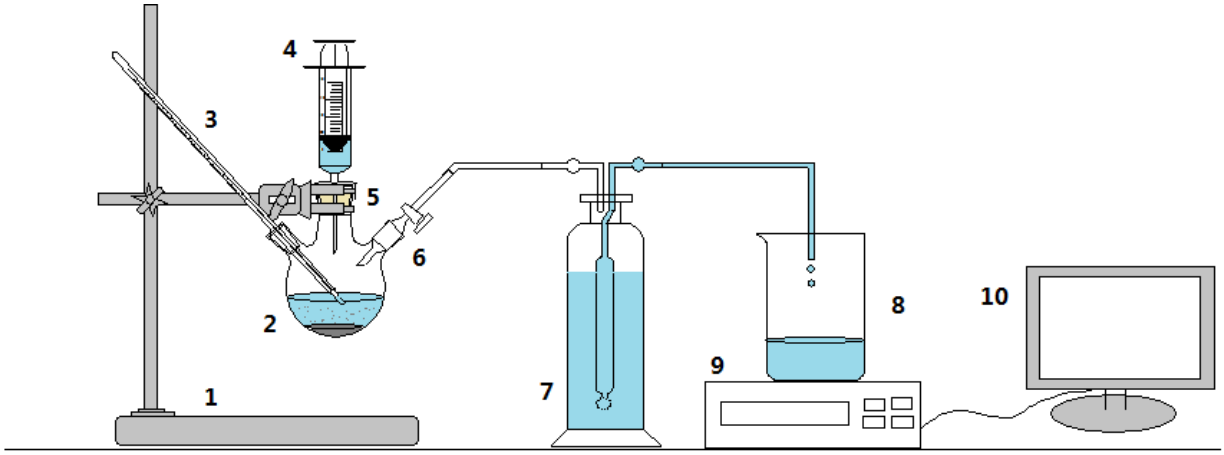

Figure 1. The schematic of equipment used to quantify hydrogen production rates and yields: (1) iron support; (2) Pyrex glass reactor; (3) thermometer; (4) injector; (5) double gum plug; (6) piston joint; (7) Monteggia washing bottle filled with water at room temperature; (8) beaker to collect the extracted water; (9) electronic scales; (10) computer.

2.3. Sample Characterization

The morphological characteristics of fabricated structures were studied by field emission scanning electron microscopy (FE-SEM, JEOL XL-30) (JEOL, Tokyo, Japan) using secondary electrons with the acceleration voltage of 10 kV, and their structural and chemical characteristics were investigated using transmission electron microscopy (TEM, JEOL-2100 (JEOL, Tokyo, Japan) equipped with an energy dispersive spectroscopy (EDS) system with an operating voltage of 200 kV).

3. Results and Discussion

3.1. Enhancement of the Hydrolysis Properties of MgH_2-Based Hydrides by Formation of a Composite Structure

The hydrolysis reaction of MgH_2 is interrupted by the formation of a magnesium hydroxide passivation layer. To improve the hydrolysis performance of MgH_2-based materials, a composite structure of MgH_2 with a different hydride was synthesized through ball milling. By adjusting the atomic ratio, MgH_2/LaH_3 composites were designed to adjust the hydrolysis performance of the MgH_2-based composite. Figure 2 shows the hydrogen production curves by hydrolysis of the MgH_2/LaH_3 composites with the different atomic ratios of 3:1, 5:1, and 8.5:1 obtained after milling for 4 h. As shown in Figure 2, the overall hydrolysis rate of the composites improved; the hydrolysis rate was the same for all the composites during the first 5 min, and then increased with the LaH_3 content. The hydrolysis of LaH_3 can produce conductive ions on the surface of the composite, which is beneficial for the work of the micro galvanic cells and results in a synergetic effect leading to a higher hydrolysis rate [65]. The

MgH_2/LaH_3 composites with the MgH_2/LaH_3 atomic ratio of 3:1 and 8.5:1 can generate 706.7 mL/g of H_2 in 40 min and 473.0 mL/g of H_2 in 60 min, respectively. The highest observed hydrolysis yield is equal to 1195 mL/g of H_2 in 80 min and belongs to the MgH_2/LaH_3 composite with the MgH_2/LaH_3 atomic ratio of 5:1. Notably, by decreasing the LaH_3 content, the hydrolysis synergetic effect was enhanced and consequently the hydrogen yield and rate increased. However, with the increase of the LaH_3 content, the theoretical hydrogen generation yield of the composites decreased because of the relatively low hydrogen yield of LaH_3.

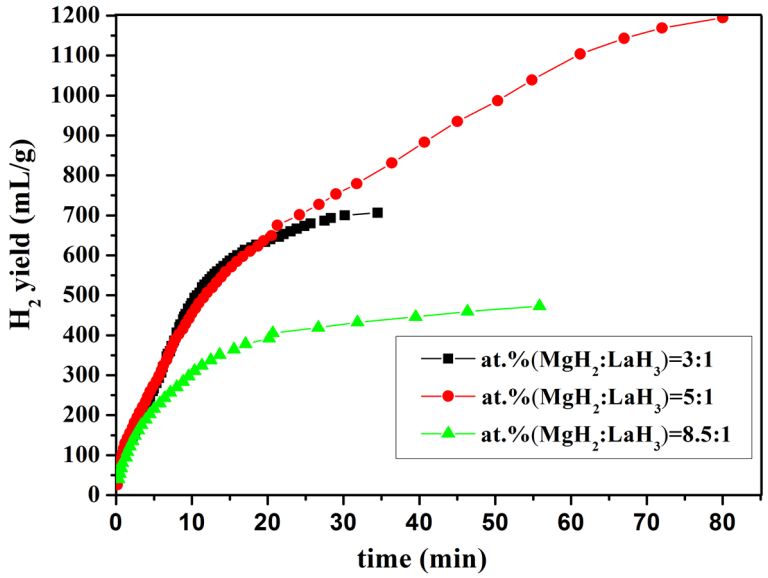

Figure 2. The hydrogen generation curves of ball-milled MgH_2 and LaH_3 with different atomic ratio.

The ball-milling method used to synthesize the composite structure of MgH_2 with other hydrides is relatively expensive, as LaH_3 and MgH_2 are obtained upon hydrogenation of Mg and La at relative high temperature. To decrease the costs of the MgH_2-based composites, an Mg-based alloy hydrogenated at room temperature with low pressure was designed. The Mg_3La and $Mg_3LaNi_{0.1}$ alloys prepared by induction melting with pure Mg and La could be hydrogenated *in situ* at room temperature and 3.8 MPa of hydrogen pressure to form the LaH_3/MgH_2 (hereafter referred to as H-Mg_3La) and $LaH_3/MgH_2/Ni$ (hereafter referred to as H-$Mg_3LaNi_{0.1}$) composites [66]. To further study the influence of the light rare earth (RE) elements on the hydrolysis performance of the composite formed *in situ*, hydrogenated Mg_3Mm (H-Mg_3Mm, Mm denotes the mischmetal), Mg_3La (H-Mg_3La), Mg_3Ce (H-Mg_3Ce), Mg_3Pr (H-Mg_3Pr), and Mg_3Nd (H-Mg_3Nd) composites were also prepared by hydrogenating the Mg_3Mm, Mg_3La, Mg_3Ce, Mg_3Pr, and Mg_3Nd (H-Mg_3Nd) alloys at 298 K [67]. The hydrolysis performances of the H-Mg_3Mm, H-Mg_3La, H-Mg_3Ce, H-Mg_3Pr, and H-Mg_3Nd composites were investigated at 298 K, as shown in Figure 3. The H-Mg_3Mm, H-Mg_3La, H-Mg_3Ce, H-Mg_3Pr, and H-Mg_3Nd composites generated 1097 mL/g, 949 mL/g, 1025 mL/g, 905 mL/g, and 657 mL/g of hydrogen by hydrolysis, with total hydrogen yields of 9.79 wt.%, 8.47 wt.%, 9.15 wt.%, 8.08 wt.%, and 5.86 wt.%, respectively.

Notably, H-Mg_3Mm exhibited the best hydrolysis performance (Figure 3, magenta line), showing the fastest hydrolysis rate and producing 695 mL/g of H_2 in 5 min, 784 mL/g of H_2 in 10 min, 828 mL/g of H_2 in 15 min, and 1097 mL/g of H_2 in 36 h. H-Mg_3La generated 463 mL/g of H_2 in 5 min and 653 mL/g

of H_2 in 10 min (Figure 3, black line). H-Mg_3Ce produced 542 mL/g of H_2 in 5 min and 705 mL/g of H_2 in 10 min (Figure 3, red line). The blue line in Figure 3 indicates the hydrolysis of the H-Mg_3Pr sample; the conversion yields were equal to 545 mL/g of H_2 in 5 min and 699 mL/g of H_2 in 10 min. For the hydrolysis of the H-Mg_3Nd sample (Figure 3, green line), the hydrolysis yield was relatively low and the sample only generated 434 mL/g of H_2 in 5 min and 581 mL/g of H_2 in 10 min. All the H-Mg_3RE samples exhibited a faster hydrolysis rate than Mg or MgH_2, indicating that the rare-earth hydrides may significantly improve the hydrolysis performance of MgH_2. For commercial use, pure rare-earth metal La was replaced by the mischmetal to reduce the costs. An inexpensive and efficient hydrolysis material, namely, as-hydrogenated Mg_3Mm (abbreviated as H-Mg_3Mm, where Mm denotes the La-rich and Ce-rich mischmetal), was identified as an excellent hydrolysis material. Pure REH_3 can fully react with water. Conversely, the hydrolysis of MgH_2 can be rapidly interrupted by the formation of a magnesium hydroxide passivation layer onto the reactive materials. During the H-Mg_3RE hydrolysis, REH_3 could continually hydrolyze and produce a reaction tunnel for the further hydrolysis of MgH_2, leading to the break of the magnesium hydroxide passivation layer. Thus, REH_3 can accelerate the hydrolysis rate of MgH_2 and lead to the completion of the hydrolysis process.

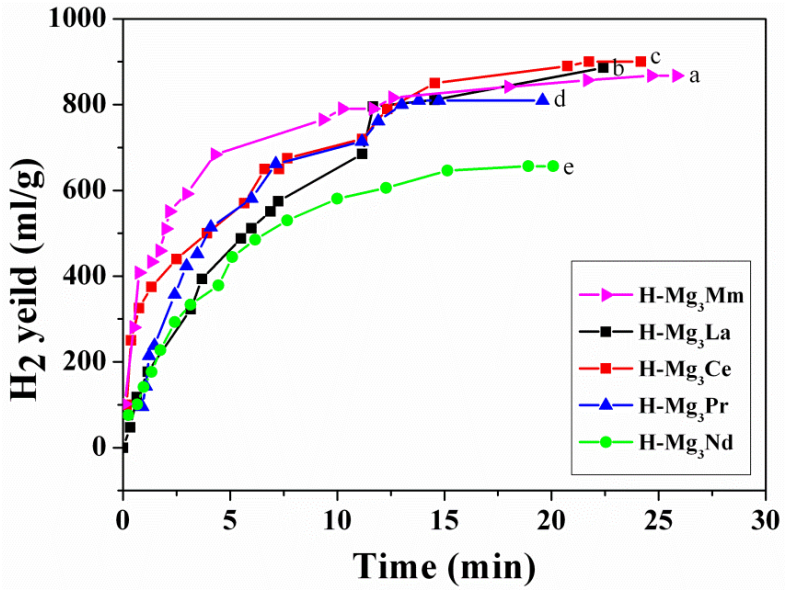

Figure 3. The hydrogen evolution curves for the hydrolysis of (a) H-Mg_3Mm; (b) H-Mg_3La; (c) H-Mg_3Ce; (d) H-Mg_3Pr and (e) H-Mg_3Nd alloys at 298 K [67]. Reproduced with permission from [67], copyright 2013 Elsevier.

Comparing the hydrogen evolution curves for the hydrolysis of the LaH_3/MgH_2 and LaH_3/MgH_2/Ni composites at room temperature (298 K), the hydrogen generation rate of LaH_3/MgH_2/Ni is higher than that of LaH_3/MgH_2 during the first 3 min [66]. The addition of Ni plays an active role in enhancing the reaction rate. However, to study the hydrolysis performance of *in situ* formed MgH_2/LaH_3 composites affected by the different atomic ratio of MgH_2 to LaH_3, MgH_2/LaH_3 composites hydrogenated from Mg_3La (MgH_2:LaH_3 = 3:1, hereafter referred to as H-Mg_3La) and La_2Mg_{17} (MgH_2:LaH_3 = 17:2, hereafter referred to as H-La_2Mg_{17}) were synthesized [47]. The results show that the hydrolysis rate of H-Mg_3La was higher than that of H-La_2Mg_{17} (918.4 mL/g and 851.7 mL/g for H-Mg_3La and H-La_2Mg_{17}, respectively, in 21 min), while the hydrogen yield decreased from 1224.5 mL/g to 983.7 mL/g in 4.4 h

for H-La_2Mg_{17} and H-Mg_3La, respectively. By increasing the content of LaH_3 from H-La_2Mg_{17} to H-Mg_3La, the interface density between the LaH_3 and MgH_2 phases significantly increased, leading a change in the rate controlling steps from a one-dimensional diffusion process to a three-dimensional interface reaction process. As the hydrolytic rate depends on the content of LaH_3, the hydrolytic rate of MgH_2 is lower than that of the hydrides in the hydrogenated La-Mg system. As a result, the kinetic properties of the LaH_3/MgH_2 composites hydrogenated from Mg_3La and La_2Mg_{17} alloys are significantly superior to those of pure MgH_2.

To further examine the composite structure, we measured the microstructure by analyzing the TEM images. As shown in Figure 4a, the bright field image of H-Mg_3Ce demonstrates the presence of MgH_2 and $CeH_{2.73}$. Figure 4b shows the selected area electron diffraction (SAED) patterns, which was obtained by selecting the diffraction spots of a circular area. The MgH_2 (PDF card 012-0697) phase with a tetragonal structure and $CeH_{2.73}$ (PDF card 089-3694) phase with an FCC structure are shown in the SAED image. A very fine plate-like or lamellar mixture of $CeH_{2.73}$ (dark) and MgH_2 (white) is observed, as identified by the SAED patterns. In the bright field image in Figure 4a, the $CeH_{2.73}$ platelet has an average width of 20 nm and a planar length of about 150 nm, whereas the MgH_2 matrix is nanocrystalline with an average grain size of approximately 20 nm. The $CeH_{2.73}$ plate is embedded in the MgH_2 phases, uniformly. The hydrolysis of $CeH_{2.73}$ can produce conductive ions on the surface of the composite results in a synergetic effect leading to a higher hydrolysis rate.

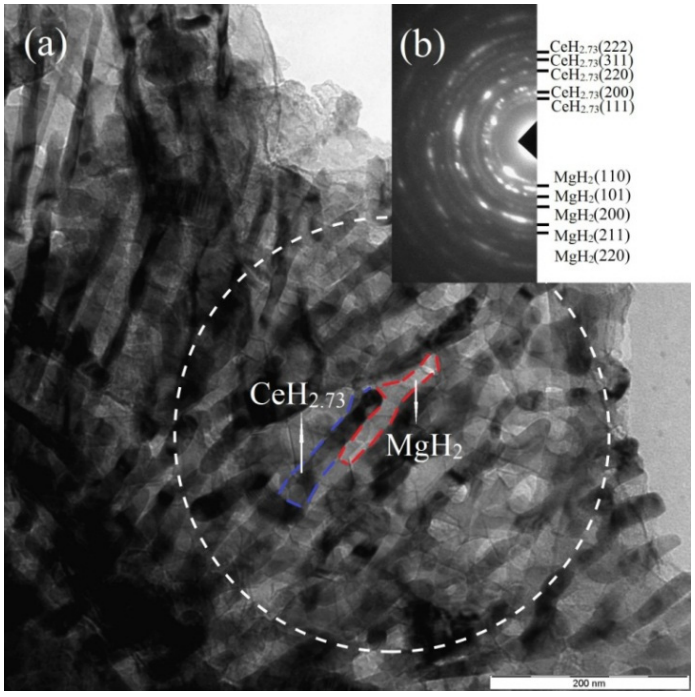

Figure 4. The bright field image of H-Mg_3Ce composite structure (**a**) and selected area diffraction patterns (**b**).

3.2. Acceleration of the Hydrolysis Reaction of MgH_2 by Controlling the Particle Size via Ball Milling

The composite structure formed via ball milling could significantly improve the hydrolysis properties. Consequently, the ball milling effect should also be investigated. Figure 5 shows the hydrogen evolution curves by hydrolysis of the as-received (untreated) and 3 h ball-milled MgH_2 in pure water. As shown

in Figure 5a, the hydrolysis rate of untreated MgH_2 in pure water is very low, and only 27.4 mL/g of H_2 could be collected in the Monteggia washing bottle after 20 min. In contrast, after 3 h ball milling, the hydrolysis rate of MgH_2 in pure water increased significantly, as shown in Figure 5b, and produced 394.6 mL/g of H_2 in 5 min. Unfortunately, the hydrolysis reaction is interrupted and there is no hydrogen produced after 5 min because of the formation of the magnesium hydroxide passivation layer. According to the hydrogen evolution curves of untreated MgH_2 and ball-milled MgH_2 in pure water by hydrolysis shown in Figure 5, the ball-milling method can effectively improve the reaction rate and yield of hydrogen generation by hydrolysis. This phenomenon could be attributed to the fact that the ball milling process refines the particle and grain size, and increases the specific surface area. In addition, the introduction of structural defects, phase change, and nanocrystalline structures is also beneficial for the MgH_2 hydrolysis. Although ball milling could improve the hydrolysis properties of MgH_2-based materials, the hydrolysis reaction of MgH_2 was still interrupted because of the formation of a magnesium hydroxide passivation layer.

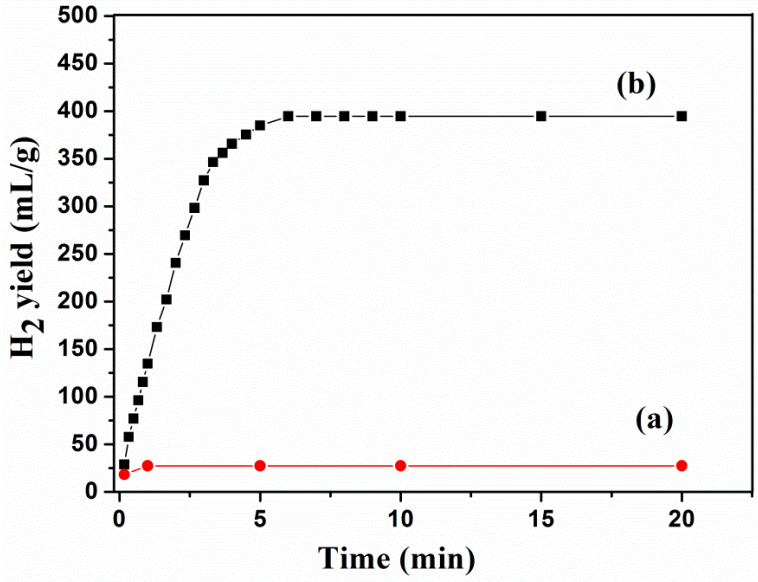

Figure 5. The hydrogen evolution curves by hydrolysis of as-received MgH_2 (a) and 3 h ball-milled MgH_2 (b) in pure water.

As a consequence, the ball-milling method has only a limited effect on the hydrolysis properties for pure MgH_2 and the MgH_2 particle size is difficult to control. To understand the effects of the particle size and ball-milling effect on the hydrolysis properties of the MgH_2-based hydrides, H-Mg_3La with different particle sizes but fixed grain sizes of LaH_3 (~17 nm) and MgH_2 (~33 nm) was prepared *in situ* by hydrogenating Mg_3La and controlling the hydrogenation conditions [68].

Figure 6 shows the hydrogen evolution curves of H-Mg_3La with different particle sizes. Clearly, the hydrolysis rate and hydrogen yield were significantly affected by the particle size. The hydrogenated Mg_3La with the smallest particle size (<12 μm) exhibited a higher hydrolysis yield of 863 mL/g (7.70 wt.%) of H_2. The final hydrogen hydrolysis yield for the samples with particle sizes of >38 μm, 38–23 μm, and 23–18 μm were 1.67 wt.%, 5.06 wt.%, and 6.26 wt.%, respectively. The smaller the particle size, the higher the observed hydrolysis rate. The above results reveal that ball milling is an effective and simple method to improve the hydrolysis properties of MgH_2-based materials.

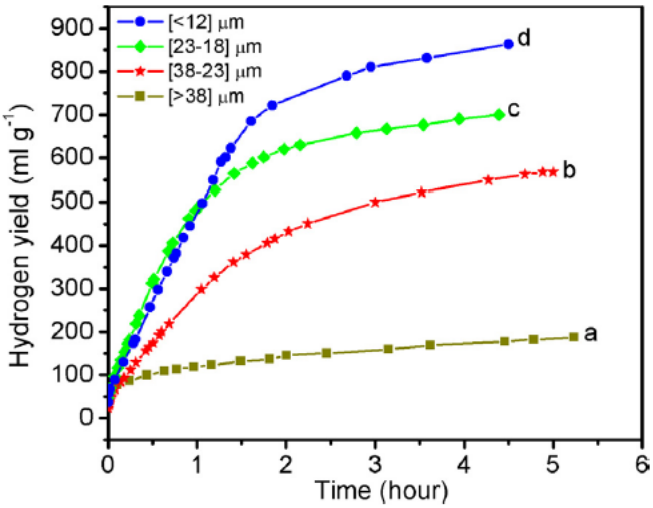

Figure 6. The hydrogen evolution curves of H-Mg_3La with different particle sizes [68]. Reproduced with permission from [68], copyright 2014 Elsevier.

Analyzing the hydrolysis curves and the hydrolysis products, we found that, as the particle size decreased, the hydrolysis rate accelerated and the hydrogen yield increased, promoting the hydrolysis of H-Mg_3La. Figure 7a,b shows the SEM images of H-Mg_3La with particle sizes >38 μm and <12 μm. The H-Mg_3La sample with particle sizes of <12 μm exhibited larger surface areas and more defects than the sample with particle size >38 μm. As the particle size decreased, the surface area and defects of the sample increased, providing larger surfaces and available sites for the water. As more contact area with water was available, the reaction proceeded more violently, preventing the magnesium hydroxide layer from covering the sample surface. The hydrolysis reaction can spontaneously continue until fully completed. Therefore, reducing the particle size is an effective and simple method to improve the hydrolysis properties of the MgH_2-based materials.

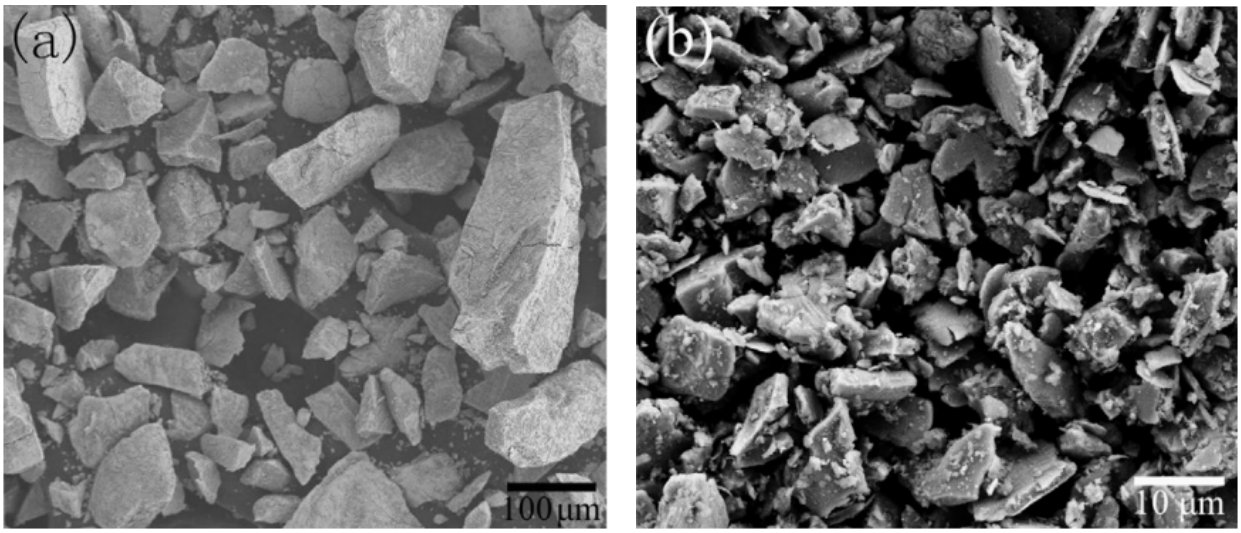

Figure 7. SEM images of H-Mg_3La with particle sizes of (**a**) [>38] μm and (**b**) [<12] μm [68]. Reproduced with permission from [68], copyright 2014 Elsevier.

3.3. Enhancement of the Hydrolysis Properties by Optimization of the Solution Composition

The hydrolysis reaction of MgH_2 can be accelerated both by controlling the particles size via ball milling and by forming composite structures. It would be significant to develop a simple method to get the high hydrolysis reaction rate of MgH_2. To break the $Mg(OH)_2$ passivation layer and accelerate the hydrolysis process, acids were used as effective hydrolytic media to enhance the hydrolysis properties. However, acids may cause corrosion damage to the reaction equipment and increase the cost of the process. The hydrolysis of MgH_2 at different concentrations of NH_4Cl aqueous solution was investigated in this work. The hydrolysis kinetics of MgH_2 at different concentrations of ammonium chloride solution is shown in Figure 8. The hydrolytic rate and hydrogen yield increased with the increase of the NH_4Cl concentration. The hydrogen evolution curves also show that the hydrogen yield kinetics of MgH_2 improved with the increase of the ammonium chloride concentration. This result confirms that the hydrolysis speed can be controlled by adjusting the solution concentration. The hydrolysis of MgH_2 produced 1711.2 mL/g of H_2 in 10 min at 298 K in the 27.1% ammonium chloride solution, and the hydrolytic conversion rate reached the value of 99.5%.

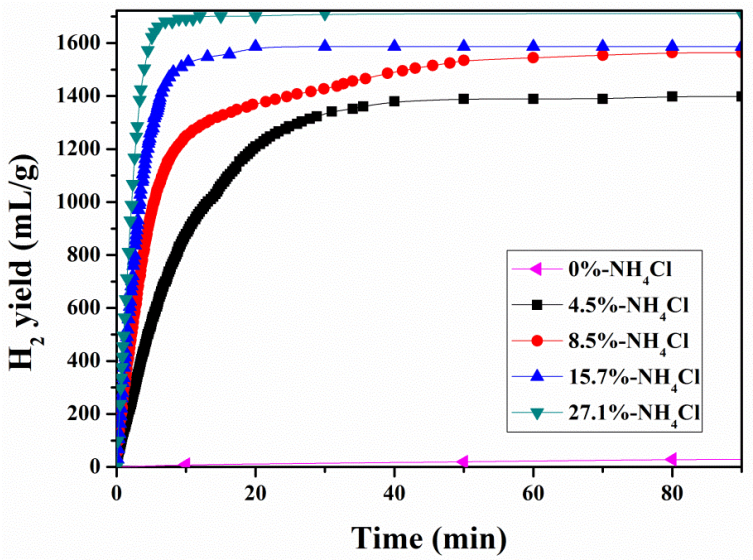

Figure 8. The hydrolysis kinetics of MgH_2 in different concentrations of ammonium chloride solution.

The introduction of a high concentration NH_4Cl solution leads to a high hydrolysis rate, but it also causes some issues, such as resource waste and equipment corrosion damage. Besides, the hydrolysis reaction in NH_4Cl solution introduces impurities and byproducts, which make the regeneration process and hydrolysis gas more complex. Thus, adding a stable catalyst to improve the hydrolysis rate may be a simple way to solve the key issue of hydrogen generation. The 0.05 mol/L $MgCl_2$ aqueous solution has been optimized for the hydrolysis of MgH_2. The hydrogen evolution curves by hydrolysis of the ball-milled MgH_2 in pure water and in a 0.05 mol/L $MgCl_2$ solution are shown in Figure 9. The hydrolysis of ball-milled MgH_2 produced 394.6 mL/g of H_2 in 5 min at 298 K, either in the $MgCl_2$ solution or in pure water, indicating that the hydrolysis rate and yield are similar in the initial stage. The hydrolysis of ball-milled MgH_2 produced 1137.4 mL/g in 90 min at 298 K in the 0.05 mol/L $MgCl_2$ solution, whereas the hydrolysis in pure water was interrupted. This result suggests that the presence of

$MgCl_2$ played a key role for the hydrolysis of MgH_2. The Mg^{2+} and Cl^- ions can actively affect the formation of a relatively loose magnesium hydroxide layer to further accelerate the hydrolysis of MgH_2 in the $MgCl_2$ solution. Furthermore, the byproduct is the MgO and $MgCl_2$ composite and no separation process is necessary for the regeneration. A simple method involves the reaction of the MgO and $MgCl_2$ composite with chlorine at 900 °C to produce $MgCl_2$; Mg can then be industrially produced by electrolysis of fused $MgCl_2$. This strategy opens a novel and effective route to modulate the hydrogen yield and hydrogen generation rate in the hydrolysis process.

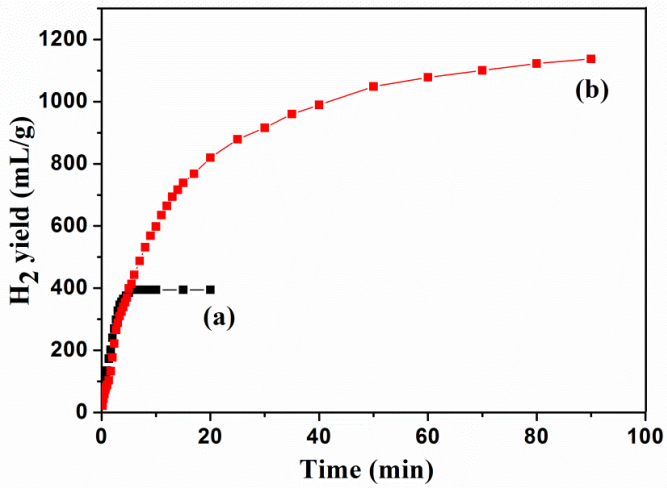

Figure 9. The hydrogen evolution curves by hydrolysis of 3 h ball-milled MgH_2 in pure water (a) and in 0.05M $MgCl_2$ solution (b).

4. Conclusions

MgH_2/LaH_3 composites were prepared by ball milling of MgH_2 and LaH_3 and showed a synergetic effect during the hydrolysis process. A low-cost method for the synthesis of MgH_2/REH_3-based composites was developed by *in situ* hydrogenation of Mg_3RE-based alloys at room temperature, and showed an enhanced hydrolysis rate. The H-Mg_3Mm, H-Mg_3La, H-Mg_3Ce, H-Mg_3Pr, and H-Mg_3Nd composites generated 1097 mL/g, 949 mL/g, 1025 mL/g, 905 mL/g, and 657 mL/g of hydrogen by hydrolysis, with the total hydrogen yields of 9.79 wt.%, 8.47 wt.%, 9.15 wt.%, 8.08 wt.%, and 5.86 wt.%, respectively. The hydrolysis properties of the MgH_2/REH_3 composites could be further adjusted by controlling the particle size via ball milling. The ammonium chloride solution, which can destroy the $Mg(OH)_2$ passivation layer and accelerate the hydrolysis process, with the MgH_2 produced 1,711.2 mL/g of H_2 in 10 min at 298 K with a hydrolytic conversion rate of 99.5%. To eliminate the impure gas and simplify the regeneration process, the 0.05 mol/L $MgCl_2$ aqueous solution was optimized for the hydrolysis of MgH_2 and the hydrogen yield was 1137.4 mL/g in 90 min at 298 K. In conclusion, MgH_2-based hydride composites, ball milling, and tuning of the solution composition are all effective methods to enhance the hydrolysis reaction rate and hydrogen generation yield of MgH_2.

Acknowledgments

This work was supported by the National Natural Science Foundation of China Projects (Nos. 51431001, U1201241 and 51271078), by Guangdong Natural Science Foundation

(2014A030311004) and by International Science and Technology Cooperation Program of China (2015DFA51750). The Project Supported by Guangdong Province Universities and Colleges Pearl River Scholar Funded Scheme (2014) is also acknowledged.

Author Contributions

Miaolian Ma, Minghong Huang, and Ruoming Duan did the experiment and collected the data; Liuzhang Ouyang and Miaolian Ma write the manuscript; Min Zhu, Hui Wang and Lixian Sun discussed the results and modified the draft.

Conflicts of Interest

The authors declare no conflict of interest.

References

1. Kikkinides, E.S. Design and optimization of hydrogen storage units using advanced solid materials: General mathematical framework and recent developments. *Comput. Chem. Eng.* **2011**, *35*, 1923–1936.
2. Bauen, A. Future energy sources and systems—Acting on climate change and energy security. *J. Power Sources* **2006**, *157*, 893–901.
3. Zhu, M.; Peng, C.H.; Ouyang, L.Z.; Tong, Y.Q. The effect of nanocrystalline formation on the hydrogen storage properties of AB_3-base Ml–Mg–Ni multi-phase alloys. *J. Alloys Compd.* **2006**, *426*, 316–321.
4. Shi, Q.; Hu, R.; Ouyang, L.; Zeng, M.; Zhu, M. High-capacity LiV_3O_8 thin-film cathode with a mixed amorphous-nanocrystalline microstructure prepared by RF magnetron sputtering. *Electrochem. Commun.* **2009**, *11*, 2169–2172.
5. Jain, I.P.; Lal, C.; Jain, A. Hydrogen storage in Mg: A most promising material. *Int. J. Hydrog. Energy* **2010**, *35*, 5133–5144.
6. Muir, S.S.; Yao, X. Progress in sodium borohydride as a hydrogen storage material: Development of hydrolysis catalysts and reaction systems. *Int. J. Hydrog. Energy* **2011**, *36*, 5983–5997.
7. Yumurtaci, Z.; Bilgen, E. Hydrogen production from excess power in small hydroelectric installations. *Int. J. Hydrog. Energy* **2004**, *29*, 687–693.
8. Gratzel, M. Perspectives for dye-sensitized nanocrystalline solar cells. *Prog. Photovolt.* **2000**, *8*, 171–185.
9. Turner, J.; Sverdrup, G.; Mann, M.K.; Maness, P.C.; Kroposki, B.; Ghirardi, M.; Evans, R.J.; Blake, D. Renewable hydrogen production. *Int. J. Energ. Res.* **2008**, *32*, 379–407.
10. Funk, J.E. Thermochemical hydrogen production: past and present. *Int. J. Hydrog. Energy* **2001**, *26*, 185–190.
11. Urbaniec, K.; Friedl, A.; Huisingh, D.; Claassen, P. Hydrogen for a sustainable global economy. *J. Clean. Prod.* **2010**, *18*, S1–S3.
12. Midilli, A.; Ay, M.; Dincer, I.; Rosen, M.A. On hydrogen and hydrogen energy strategies: I: Current status and needs. *Renew. Sustain. Energy Rev*. **2005**, *9*, 255–271.

13. Demirci, U.B.; Miele, P. Overview of the relative greenness of the main hydrogen production processes. *J. Clean. Prod.* **2013**, *52*, 1–10.
14. Ersoz, A.; Olgun, H.; Ozdogan, S. Reforming options for hydrogen production from fossil fuels for PEM fuel cells. *J. Power Sources* **2006**, *154*, 67–73.
15. Das, D.; Veziroglu, T.N. Advances in biological hydrogen production processes. *Int. J. Hydrog. Energy* **2008**, *33*, 6046–6057.
16. Balachandran, U.; Dorris, S.E.; Bose, A.C.; Stiegel, G.J.; Lee, T.H. Method of generating hydrogen by catalytic decomposition of water. U.S. Patent US6468499 B1, 22 November 2002.
17. Hiraki, T.; Hiroi, S.; Akashi, T.; Okinaka, N.; Akiyama, T. Chemical equilibrium analysis for hydrolysis of magnesium hydride to generate hydrogen. *Int. J. Hydrog. Energy* **2012**, *37*, 12114–12119.
18. Ni, M.; Leung, D.Y.C.; Leung, M.K.H.; Sumathy, K. An overview of hydrogen production from biomass. *Fuel Process. Technol.* **2006**, *87*, 461–472.
19. Holladay, J.D.; Hu, J.; King, D.L.; Wang, Y. An overview of hydrogen production technologies. *Catal. Today* **2009**, *139*, 244–260.
20. Manish, S.; Banerjee, R. Comparison of biohydrogen production processes. *Int. J. Hydrog. Energy* **2008**, *33*, 279–286.
21. Antal, T.K.; Krendeleva, T.E.; Rubin, A.B. Acclimation of green algae to sulfur deficiency: underlying mechanisms and application for hydrogen production. *Appl. Microbiol. Biotechnol.* **2011**, *89*, 3–15.
22. Basak, N.; Das, D. The Prospect of Purple Non-Sulfur (PNS) photosynthetic bacteria for hydrogen production: The present state of the art. *World J. Microbiol. Biotechnol.* **2007**, *23*, 31–42.
23. Huesemann, M.H.; Hausmann, T.S.; Carter, B.M.; Gerschler, J.J.; Benemann, J.R. Hydrogen generation through indirect biophotolysis in batch cultures of the nonheterocystous nitrogen-fixing cyanobacterium plectonema boryanum. *Appl. Biochem. Biotechnol.* **2010**, *162*, 208–220.
24. Xie, G.J.; Liu, B.F.; Ding, J.; Ren, H.Y.; Xing, D.F.; Ren, N.Q. Hydrogen production by photo-fermentative bacteria immobilized on fluidized bio-carrier. *Fuel Energy Abstr.* **2011**, *36*, 13991–13996.
25. Kovács, K.L.; Maróti, G.; Rákhely, G. A novel approach for biohydrogen production. *Int. J. Hydrog. Energy* **2006**, *31*, 1460–1468.
26. Laurinavichene, T.; Kosourov, S.; Ghirardi, M.; Seibert, M.; Tsygankov, A. Prolongation of H_2 photoproduction by immobilized, sulfur-limited Chlamydomonas reinhardtii cultures. *J. Biotechnol.* **2008**, *134*, 275–277.
27. Hydrogen, Fuel Cells and Infrastructure Technologies Program Multi-Year Research, Development and Demonstration Plan. Available online: http://www.nrel.gov/docs/fy08osti/39146.pdf (accessed on 5 May 2015).
28. Levin, D.B.; Pitt, L.; Love, M. Biohydrogen production: Prospects and limitations to practical application. *Int. J. Hydrog. Energy* **2004**, *29*, 173–185.
29. Bhandari, R.; Trudewind, C.A.; Zapp, P. Life cycle assessment of hydrogen production via electrolysis—A review. *J. Clean. Prod.* **2014**, *85*, 151–163.
30. Janssen, H.; Bringmann, J.C.; Emonts, B.; Schroeder, V. Safety-related studies on hydrogen production in high-pressure electrolysers. *Int. J. Hydrog. Energy* **2004**, *29*, 759–770.
31. Koroneos, C.; Dompros, A.; Roumbas, G.; Moussiopoulos, N. Life cycle assessment of hydrogen fuel production processes. *Int. J. Hydrog. Energy* **2004**, *29*, 1443–1450.

32. Fujishima, A.; Honda, K. Electrochemical photolysis of water at a semiconductor electrode. *Nature* **1972**, *238*, 37–38.
33. Liu, G.; Shi, J.; Zhang, F.; Chen, Z.; Han, J.; Ding, C.; Chen, S.; Wang, Z.; Han, H.; Li, C. A tantalum nitride photoanode modified with a hole-storage layer for highly stable solar water splitting. *Angew. Chem.* **2014**, *53*, 7295–7299.
34. Aroutiounian, V.M.; Arakelyan, V.M.; Shahnazaryan, G.E. Metal oxide photoelectrodes for hydrogen generation using solar radiation-driven water splitting. *Sol. Energy* **2005**, *78*, 581–592.
35. Wang, H.Z.; Leung, D.Y.C.; Leung, M.K.H.; Ni, M. A review on hydrogen production using aluminum and aluminum alloys. *Renew. Sustain. Energ. Rev.* **2009**, *13*, 845–853.
36. Aleksandrov, Y.A.; Tsyganova, E.I.; Pisarev, A.L. Reaction of Aluminum with Dilute Aqueous NaOH Solutions. *Russ. J. Gen. Chem.* **2003**, *73*, 689–694.
37. Soler, L.; Candela, A.M.; Macanás, J.; Muñoz, M.; Casado, J. *In situ* generation of hydrogen from water by aluminum corrosion in solutions of sodium aluminate. *J. Power Sources* **2009**, *192*, 21–26.
38. Soler, L.; Candela, A.M.; Macanás, J.; Muñoz, M.; Casado, J. Hydrogen generation from water and aluminum promoted by sodium stannate. *Int. J. Hydrog. Energy* **2010**, *35*, 1038–1048.
39. Alinejad, B.; Mahmoodi, K. A novel method for generating hydrogen by hydrolysis of highly activated aluminum nanoparticles in pure water. *Int. J. Hydrog. Energy* **2009**, *34*, 7934–7938.
40. Deng, Z.Y.; Liu, Y.F.; Tanaka, Y.; Ye, J.; Sakka, Y. Modification of Al Particle Surfaces by γ-Al_2O_3 and Its Effect on the Corrosion Behavior of Al. *J. Am. Ceram. Soc.* **2005**, *88*, 977–979.
41. Huang, T.; Gao, Q.; Liu, D.; Xu, S.; Guo, C.; Zou, J.; Wei, C. Preparation of Al-Ga-In-Sn-Bi quinary alloy and its hydrogen production via water splitting. *Int. J. Hydrog. Energy* **2015**, *40*, 2354–2362.
42. Kong, V.C.Y.; Foulkes, F.R.; Kirk, D.W.; Hinatsu, J.T. Development of hydrogen storage for fuel cellgenerators. I: Hydrogen generation using hydrolysishydrides. *Int. J. Hydrog. Energy* **1999**, *24*, 665–675.
43. Beattie, S.D.; Langmi, H.W.; McGrady, G.S. *In situ* thermal desorption of H_2 from $LiNH_2$–2LiH monitored by environmental SEM. *Int. J. Hydrog. Energy* **2009**, *34*, 376–379.
44. Ward, C.A.; Stanga, D.; Pataki, L.; Venter, R.D. Design for the cold start-up of a man-portable fuel cell and hydrogen storage system. *J. Power Sources* **1993**, *41*, 335–352.
45. Grosjean, M.H.; Roué, L. Hydrolysis of Mg-salt and MgH_2-salt mixtures prepared by ball milling for hydrogen production. *J. Alloys Compd.* **2006**, *416*, 296–302.
46. Lukashev, R.V.; Yakovleva, N.A.; Klyamkin, S.N.; Tarasov, B.P. Effect of mechanical activation on the reaction of magnesium hydride with water. *Russ. J. Inorg. Chem.* **2008**, *53*, 343–349.
47. Ouyang, L.Z.; Xu, Y.J.; Dong, H.W.; Sun, L.X.; Zhu, M. Production of hydrogen via hydrolysis of hydrides in Mg–La system. *Int. J. Hydrog. Energy* **2009**, *34*, 9671–9676.
48. Zhao, Z.; Zhu, Y.; Li, L. Efficient catalysis by $MgCl_2$ in hydrogen generation via hydrolysis of Mg-based hydride prepared by hydriding combustion synthesis. *Chem. Commun.* **2012**, *48*, 5509–5511.
49. Kojima, Y.; Haga, T. Recycling process of sodium metaborate to sodium borohydride. *Int. J. Hydrog. Energy* **2003**, *28*, 989–993.
50. Demirci, U.B.; Akdim, O.; Miele, P. Ten-year efforts and a no-go recommendation for sodium borohydride for on-board automotive hydrogen storage. *Int. J. Hydrog. Energy* **2009**, *34*, 2638–2645.

51. Stearns, J.E.; Matthews, M.A.; Reger, D.L.; Collins, J.E. The thermal characterization of novel complex hydrides. *Int. J. Hydrog. Energy* **1998**, *23*, 469–474.
52. Aiello, R.; Sharp, J.H.; Matthews, M.A. Production of hydrogen from chemical hydrides via hydrolysis with steam. *Int. J. Hydrog. Energy* **1999**, *24*, 1123–1130.
53. Kojima, Y. Hydrogen generation by hydrolysis reaction of lithium borohydride. *Int. J. Hydrog. Energy* **2004**, *29*, 1213–1217.
54. Kato, Y.; Sasaki, Y.; Yoshizawa, Y. Magnesium oxide/water chemical heat pump to enhance energy utilization of a cogeneration system. *Energy* **2005**, *30*, 2144–2155.
55. Uan, J.Y.; Yu, S.H.; Lin, M.C.; Chen, L.F.; Lin, H.I. Evolution of hydrogen from magnesium alloy scraps in citric acid-added seawater without catalyst. *Int. J. Hydrog. Energy* **2009**, *34*, 6137–6142.
56. Huot, J.; Liang, G.; Schulz, R. Magnesium-based nanocomposites chemical hydrides. *J. Alloys Compd.* **2003**, *353*, L12–L15.
57. Cho, C.Y.; Wang, K.H.; Uan, J.Y. Evaluation of a new hydrogen generating system: Ni-Rich magnesium alloy catalyzed by platinum wire in sodium chloride solution. *Mater. Trans.* **2005**, *46*, 2704–2708.
58. Uan, J.Y.; Cho, C.Y.; Liu, K.T. Generation of hydrogen from magnesium alloy scraps catalyzed by platinum-coated titanium net in NaCl aqueous solution. *Int. J. Hydrog. Energy* **2007**, *32*, 2337–2343.
59. Uan, J.Y.; Lin, M.C.; Cho, C.Y.; Liu, K.T.; Lin, H.I. Producing hydrogen in an aqueous NaCl solution by the hydrolysis of metallic couples of low-grade magnesium scrap and noble metal net. *Int. J. Hydrog. Energy* **2009**, *34*, 1677–1687.
60. Grosjean, M.H.; Zidoune, M.; Huot, J.Y.; Roué, L. Hydrogen generation via alcoholysis reaction using ball-milled Mg-based materials. *Int. J. Hydrog. Energy* **2006**, *31*, 1159–1163.
61. Grosjean, M.H.; Zidoune, M.; Roué, L.; Huot, J.Y. Hydrogen production via hydrolysis reaction from ball-milled Mg-based materials. *Int. J. Hydrog. Energy* **2006**, *31*, 109–119.
62. Hiroi, S.; Hosokai, S.; Akiyama, T. Ultrasonic irradiation on hydrolysis of magnesium hydride to enhance hydrogen generation. *Int. J. Hydrog. Energy* **2011**, *36*, 1442–1447.
63. Tessier, J.P.; Palau, P.; Huot, J.; Schulz, R.; Guay, D. Hydrogen production and crystal structure of ball-milled MgH_2–Ca and MgH_2–CaH_2 mixtures. *J. Alloys Compd.* **2004**, *376*, 180–185.
64. Izumi, F.; Ikeda, T. A rietveld-analysis programm RIETAN-98 and its applications to zeolites. *Mater. Sci. Forum.* **2000**, *321–324*, 198–205.
65. Fan, M.Q.; Xu, F.; Sun, L.X.; Zhao, J.N.; Jiang, T.; Li, W.X. Hydrolysis of ball milling Al–Bi–hydride and Al–Bi–salt mixture for hydrogen generation. *J. Alloys Compd.* **2008**, *460*, 125–129.
66. Ouyang, L.Z.; Wen, Y.J.; Xu, Y.J.; Yang, X.S.; Sun, L.X.; Zhu, M. The effect of Ni and Al addition on hydrogen generation of Mg_3La hydrides via hydrolysis. *Int. J. Hydrog. Energy* **2010**, *35*, 8161–8165.
67. Ouyang, L.Z.; Huang, J.M.; Wang, H.; Wen, Y.J.; Zhang, Q.A.; Sun, D.L.; Zhu, M. Excellent hydrolysis performances of Mg_3RE hydrides. *Int. J. Hydrog. Energy* **2013**, *38*, 2973–2978.
68. Huang, J.M.; Duan, R.M.; Ouyang, L.Z.; Wen, Y.J.; Wang, H.; Zhu, M. The effect of particle size on hydrolysis properties of Mg_3La hydrides. *Int. J. Hydrog. Energy* **2014**, *39*, 13564–13568.